Soft Matter

PAPER

View Article Online
View Journal | View Issue

Cite this: *Soft Matter*, 2025, **21**, 2251

Synthesis and isolation of metalloprotein on a super water-repellent umbrella-shaped pillar array with double re-entrant structure

Daiki Tanaka, *[a] Masashi Kobayashi,[a] Risa Fujita,[b] Dong Hyun Yoon, [bc] Tetsushi Sekiguchi,[b] Takashiro Akitsu,[d] Shuichi Shoji,[a] Takashi Tanii[a] and Masahiro Furuya[a]

Received 11th November 2024,
Accepted 17th February 2025

DOI: 10.1039/d4sm01334d

rsc.li/soft-matter-journal

This paper reports the generation of microdroplets on a water-repellent device equipped with an array of tiny umbrella-shaped pillar structures. The microdroplets were used for chemical synthesis, docking, and crystallization of a functional protein. The umbrella-shaped water-repellent devices were easily fabricated from SU-8 by soft micro-electromechanical systems technology, which would suit mass production. We used simulations to visually clarify how water and methanol were repelled and quantitatively determined the umbrella-shaped structure's water-repellency by measuring a microdroplet's contact angle. Pillar array devices reduce the amount of reagents used in chemical synthesis experiments and facilitate chemical analysis. Furthermore, the reaction speed in microdroplets is often faster. The synthesis of a Zn(II) complex, which usually takes 4 h in a beaker, was completed in less than 120 s. The reaction inside the microdroplets was observed with a high-speed camera, and the products were identified by optical analysis. A metal complex and protein were docked and crystallized in microdroplets on the water-repellent device. The crystallization was observed under an optical microscope, producing beautiful single protein crystals. The metal complex and protein docking was confirmed by elemental analysis of the crystals.

Introduction

Functional proteins such as lysozymes containing a Zn(II) complex are expected to be used in diverse applications, including tumour markers and fuel cell electrodes.[1–4] For example, Das *et al.*[5] and Fani *et al.*[6] reported functional complexes that exhibit antimycobacterial activity against *Mycobacterium tuberculosis* strains. These complexes have low toxicity to healthy cells and thus are promising for drug discovery. Furthermore, Nogala *et al.* reported laccase's oxidation–reduction potential, using laccase and $[Fe(CN)_6]^{3-/4-}$ as a mediator to build a biologically safe biofuel cell.[7]

Crystallization of functional proteins is important for clarifying their structure and characteristics. However, a stable crystallization technique for functional proteins has not yet been established. In recent years, microfluidic devices have been investigated for crystallizing functional proteins.[8–10] For example, Maeki *et al.* controlled the shape of crystals by changing the size of the crystallization chamber.[11] Maeki *et al.* also performed structural analysis by exposing protein crystals inside the microfluidic device to X-rays.[12] Ferreira *et al.* used thermodynamics and kinetics to explain how droplet volume and interface differences affect protein crystallization.[13] Zhu *et al.* developed an automated robotic system for nanolitre-scale protein crystallization screening, which reduced protein consumption by 50–500 times.[14] Microdroplet crystallization has also been used for things other than proteins.[15] For example, J. Jang *et al.* investigated the effect of solution volume on the chiral symmetry breaking (CSB) phenomenon in enantiomeric sodium chlorate crystals.[16]

Chemical reactions on a microscale can show increased efficiency.[17–23] For example, Kim *et al.* developed a microfluidic technique to overcome the extremely rapid anionic Fries rearrangement for the chemoselective functionalization of the *ortho* position of iodophenyl carbamates.[24] Fukuda *et al.* developed a real-time method to monitor the reaction of 5(6)-carboxynaphthofluorescein succinimidyl ester with CdSe/ZnS quantum dots using microdroplets formed in a microfluidic device.[25] Neumann *et al.* developed microflow conditions for visible light photoredox catalysis and demonstrated that the productivity of enantioselective photoredox α-alkylation increased by two orders of magnitude.[26]

[a] *Faculty of Science and Engineering, Waseda University, Tokyo 169-8555, Japan. E-mail: d.tanaka@ruri.waseda.jp*
[b] *Research Organization for Nano & Life Innovation, Waseda University, Tokyo 162-0041, Japan*
[c] *Research Institute of Industrial Science & Technology (RIST), Pohang, 37673, Republic of Korea*
[d] *Department of Chemistry, Faculty of Science, Tokyo University of Science, Tokyo 162-8601, Japan*

Protein crystallization and chemical synthesis have been performed using microfluidic devices, but protein crystals and solid products can get stuck in the flow channels and are difficult to remove from the microfluidic device. We have conducted lysozyme crystallization experiments in microdroplets using a microfluidic device. Although lysozyme crystallized in the microdroplets, the crystals were easily broken when we picked them up or removed them from the closed devices. Therefore, we devised a simple crystallization method using an open-air water-repellent structure.

Various water-repellent devices have been investigated.[27–30] Su *et al.* reported a small droplet reactor that exploited a nanoparticle-derived superhydrophobic pedestal's wettability and low adhesion. This not only allows the water droplets to be manipulated freely but also provides a closed environment to perform a series of water-phase chemical reactions.[31] Luo *et al.* developed a water-repellent material with high wear resistance by spraying Cu particles onto a substrate. The material may have various outdoor applications for self-cleaning and corrosion protection of metal parts.[32] Water-repellent devices that use micro-electromechanical systems (MEMS) technology have also been devised.[33–35] Liu *et al.* reported using 3D printing to create a fine umbrella-shaped structure that exhibited liquid repellence against organic solvents.[36] Oyunbaatar *et al.* fabricated a microscopic pillar array device using polydimethylsiloxane (PDMS) and used the device to observe cardiomyocytes.[37] Fujii *et al.* also investigated the characteristics of lysozyme crystallization on fractal surfaces.[38] Chemical reactions have also been carried out using water-repellent devices.[39] K. Li *et al.* carried out oxidation reactions of methyl orange, golden orange II, and levoglucosan using Fe(III)-oxalic acid photochemistry and g-C_3N_4 photocatalysis in microdroplets on a water-repellent device, and observed the interfacial concentration and pH changes in the microdroplets using Raman scattering microscopy.[40]

Many kinds of liquid-repellent structures and materials have been reported. Among them, the double re-entrant structure has shown the best repellent performance. Double re-entrant structures are characterized by their unique geometry, which includes both horizontal and vertical overhangs. These structures are engineered to enhance liquid repellency, making them particularly effective against a wide range of liquids, including those with low surface tension, when employing only structural features.[41] This structure guarantees that liquids form spherical droplets, and thus, a large proportion of the liquid can participate in the reaction, even though the droplet has a small volume and high wettability on the surface. Furthermore, the open structure allows simple experimental procedures for adding reagents and collecting crystals.

In this study, we used the umbrella pillar double re-entrant structure as a liquid-repellent structure (Fig. 1). The production process was simplified using photosensitive resin (SU-8) and PDMS as device materials. Traditional 3D printing is lengthy, but the device developed in this study can be mass-produced quickly. The device is flexible due to the characteristics of the material. In addition, chemical synthesis and protein crystallization were performed. Fig. 2 shows an overview of this work. Organic solvent and water microdroplets were generated on the water-repellent device, the chemical synthesis and protein crystallization were carried out in the microdroplets, and the products were collected easily with a pipette.

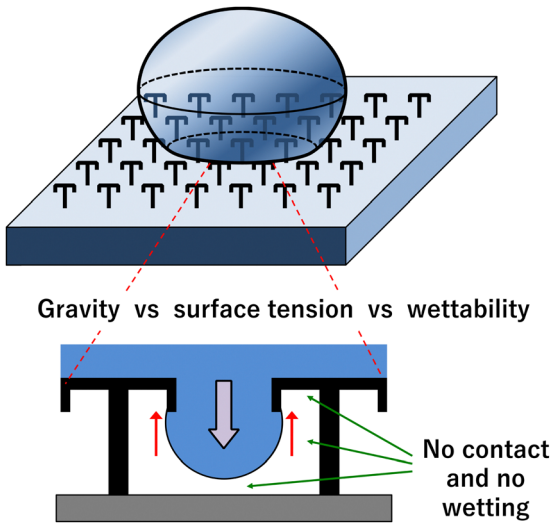

Fig. 1 Conceptual diagram of the pillar array device (top) and the principle of water repellence (bottom).

Experimental

Materials

The chemicals and reagents were of the highest grade commercially available (Tokyo Chemical Industry; Kanto Chemical) and used as received without further purification.

Fabrication process

In this study, SU-8 (3050, 3025, and 3005, Kayaku MicroChem), a photosensitive resin with high chemical resistance, was used

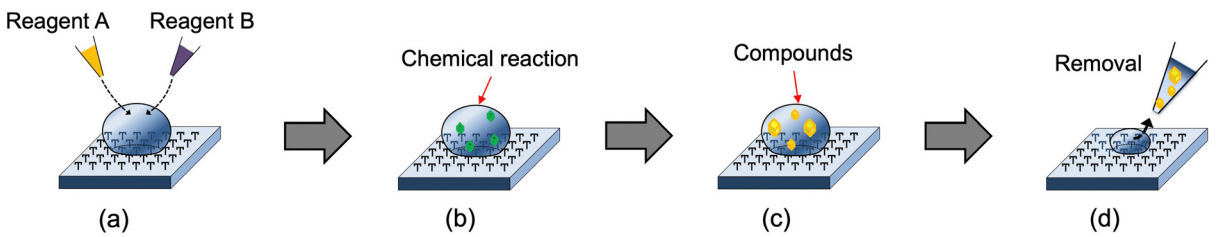

Fig. 2 Overview of chemical synthesis and crystallization experiments using pillar array devices. (a) Dropping of reagent and generation of microdroplets. (b) Highly efficient chemical synthesis. (c) Precipitation of the target compound. (d) Removal of compounds using a pipette.

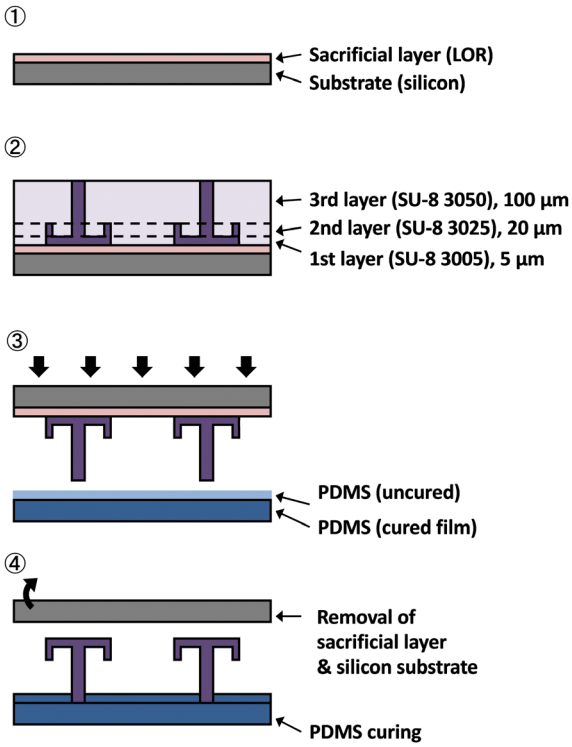

Fig. 3 Fabrication of the umbrella-shaped pillar device. 1. Sacrificial layer application. 2. Three-step SU-8 coating and patterning. 3. Development and bonding to PDMS. 4. Curing of PDMS and removal of the sacrificial layer.

to fabricate a water-repellent device for chemical synthesis. The fabrication process is shown in Fig. 3.

(1). The Si substrate was coated with the sacrificial layer (lift-off resist) and pre-baked at 90 °C for 5 min.

(2). SU-8 3005 was spin-coated to a thickness of 5 μm, prebaked at 95 °C for 5 min, and patterned by using a UV exposure machine (MA/BA6, SUSS MicroTec). SU-8 3025 was spin-coated to a thickness of 20 μm, prebaked at 95 °C for 10 min, and patterned using the UV exposure machine. SU-8 3050 was spin-coated to a thickness of 100 μm, prebaked at 95 °C for 30 min, and patterned by using the UV exposure machine. Finally, all three layers were developed with an SU-8 developer.

(3). A 10–20-μm-thick layer of uncured PDMS was applied to the cured PDMS sheet by spin coating. The patterning device prepared in process 2 was pressed onto the PDMS surface, and the PDMS was baked at 120 °C for 60 min.

(4). The device was submerged in water to dissolve the sacrificial layer. The water-repellent device was slowly removed from the Si substrate and then dried on a hot plate at 80 °C for 60 min.

Fig. 4(a) shows the dimensions of the umbrella-shaped part of the water-repellent device. The diameter of the umbrella was 60 μm, and the height was 125 μm. The spacing between the pillars was 150 μm. Fig. 4(b) and (c) shows an optical microscope image of the pillar array and a photograph of the water-repellent device. The micrograph of the surface of the

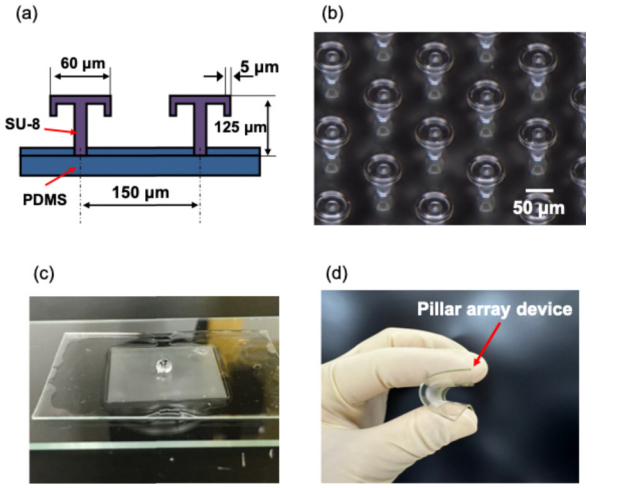

Fig. 4 Dimensions and appearance of pillar array device. (a) Device dimensions. The umbrella diameter is 60 μm and the distance between pillars is 150 μm. (b) Micrograph of the umbrella-shaped pillars made of SU-8. (c) Photograph of a water drop on the umbrella-shaped pillar device. (d) Flexibility of pillar array devices.

umbrella-shaped pillar array device confirms that the umbrella-shaped pillars made of SU-8 were neatly fabricated (Fig. 4(b)). The photograph of the umbrella-shaped pillar array device shows that the device repelled water (Fig. 4(c)). The SU-8 pillar array was arranged on a PDMS sheet and was flexible because the array was also made of PDMS (Fig. 4(d)). PDMS and SU-8 have high chemical resistance, making them well suited for chemical synthesis and biochemical experiments. The micro-droplets on the water-repellent substrate could be moved by tilting the substrate by 30–45°.

Simulation of water-repellent device

Computational fluid dynamics simulations (STAR-CCM+ version 2310, Siemens) were conducted to analyze the behavior of droplets between pillars. Two simulation cases were examined, with either a methanol or a water droplet on the pillars. The contact angle of methanol on the pillar surface was 22.3°, whereas that of water was 91.7°. These values were estimated based on the contact angles of methanol and water on SU-8 as the substrate material.

Measuring the contact angle of water-repellent devices

The dropping method measured the contact angles of water and methanol on a water-repellent substrate with a contact angle meter (DropMaster 500, Kyowa Interface Science Co., Ltd.). The contact angle was measured for a substrate coated with SU-8 and for an umbrella-shaped pillar array. The SU-8 substrate was baked, exposed, and developed.

Synthesis of a Zn(II) complex

Fig. 5 shows a synthesis scheme for the Zn(II) complex. All steps of synthesizing the Zn(II) complex were carried out on a pillar array water-repellent device. The Zn(II) complex was synthesized in two steps. In step 1, the ligand was synthesized. 3,5-Dichlorosalicylaldehyde (40 mmol L^{-1}, methanol solvent) was added

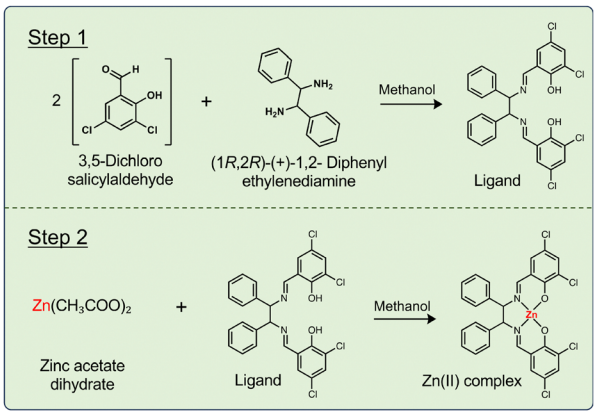

Fig. 5 Synthesis scheme of the Zn(II) complex. Step 1: Synthesis of the ligand from 3,5-dichlorosalicylaldehyde and (1*R*,2*R*)-(+)-1,2-diphenyl-ethylene-diamine. Step 2: Synthesis of the Zn(II) complex from the ligand and zinc acetate.

dropwise to a solution droplet of (1*R*,2*R*)-(+)-1,2-diphenylethylene-diamine (20 mmol L^{-1}, methanol solvent). The two solutions were mixed and left for 120 s to synthesize the ligand. In step 2, zinc acetate hydrate (20 mmol L^{-1}, methanol solvent) was added dropwise to the synthesized ligand droplets. The solutions were mixed and left for 120 s to synthesize the Zn(II) complex. The reaction was observed under an optical microscope. The synthesis product was easily recovered using a pipette. Identification analysis was carried out using ultraviolet-visible (UV-vis) spectroscopy (V-630, JASCO) and infrared (IR) spectroscopy (FT/IR-6200, JASCO). Furthermore, the products in the beaker and droplets were diluted 40 times and the yields were compared based on the UV-vis peak intensity.

Synthesis and crystallization of a Zn(II) complex-containing protein

All steps of synthesizing and crystallizing a metal complex-containing protein were carried out on a water-repellent device. Fig. 6 shows the protein and metal complex solutions being dropped with a pipette. The crystallization experiment was carried out using the Zn(II) complex (8 mmol L^{-1}) and lysozyme (10 mmol L^{-1}). Each reagent was dissolved in an aqueous citrate buffer solution. The aqueous solutions were dropped and mixed on an umbrella pillar array by pipettes, and the crystallization experiment was conducted at room temperature (23 °C) under ambient conditions. During the crystallization experiments, the dropped microdroplets were covered with small lids to prevent evaporation of the solution. The crystallization time was varied from 0 to 120 min. The crystallization was observed periodically with an optical microscope immediately after dropwise mixing. Crystallized materials were picked up with a pipette and washed with pure water. The crystals were analysed by scanning electron microscopy (SEM; SU8240, Hitachi) and energy-dispersive X-ray spectroscopy (EDX; Genesis-AP2, EDAX).

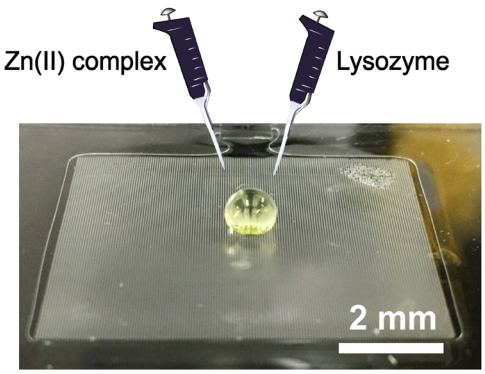

Fig. 6 Overview of crystallization experiment. Zn(II) complex and lysozyme were added dropwise and left for 120 min after the formation of the microdroplets.

Results and discussion

Simulation of water-repellent device

Fig. 7 shows the results of a two-dimensional computational fluid dynamics simulation of a droplet on micro-structured pillars. The air–droplet interface shown in Fig. 7 indicates a range of VOF values between 0.45 and 0.55. The mesh size used in the analysis was 500 nm and the time step for the unsteady analysis was 100 ns. The results indicated that even liquids with low contact angles, such as methanol, cannot completely wet the pillars; furthermore, the interface shape between the pillars differed between the two liquids. In methanol, the interface existed at the bottom of the pillar, whereas in water the interface was at the top of the pillar and the interface was horizontal. This difference was attributed to the variations in surface tension and contact angle between methanol and water. Water, which has a higher surface tension than methanol, tends to minimize its surface area, resulting in a flatter interface. Additionally, the larger contact angle of water increased the angle between the two ends where the liquid was in contact with the pillar by nearly 90°.

Measuring the contact angle of water-repellent devices

Fig. 8 compares the contact angles of a water-repellent device (made of SU-8) and an SU-8 substrate. The solvents used in this study were water and methanol, so the contact angles of the two liquids were measured. When comparing the SU-8 substrate with the umbrella-shaped water-repellent device, the change in the orientation of the substrate changed from 91.7° to 137.3° for water, and from 22.3° to 118.8° for methanol. The SU-8 substrate has water-repellent properties, so the contact angle was over 90°, but the umbrella-shaped water-repellent device

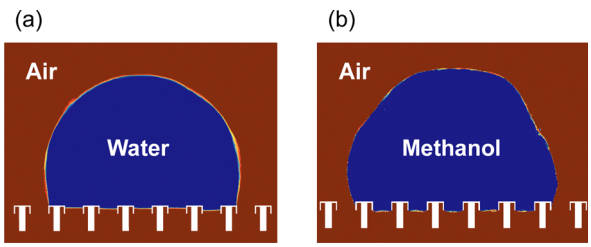

Fig. 7 Simulation of droplet shape on an umbrella-shaped water-repellent device. (a) Water microdroplet. (b) Methanol microdroplet.

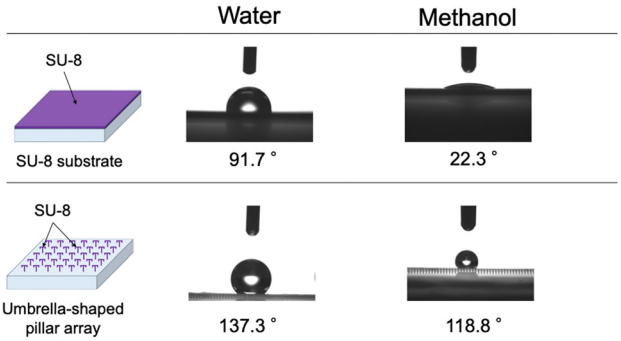

Fig. 8 Contact angles for the water-repellent device and an SU-8 substrate with water and methanol (n = 10).

had an even larger contact angle. Methanol could not form droplets on a SU-8 substrate because it can wet SU-8 and has a small surface tension. In contrast, on the umbrella-shaped water-repellent device, methanol had a large contact angle of 118.8° and formed microdroplets. Furthermore, when the umbrella-shaped water-repellent device was tilted by about 30°, the droplets rolled off and could be collected easily. The ease with which the droplets moved was attributed to the umbrella-shaped pillars with air underneath. The droplets could also be collected with a pipette. On the other hand, the methanol on the flat SU-8 substrate spread and could not be collected with a pipette. The water-repellent device is reusable, and water droplets can be formed any number of times, but if the pillars are damaged by physical force, the water-repellent ability is lost.

Synthesis of a Zn(II) complex

Fig. 9 shows a high-speed camera image of a chemical reaction. The Zn(II) complex formation in step 2 was observed (Fig. 5). The chemical reaction in step 2 involves mixing the ligand (liquid) with zinc acetate (liquid) to produce a solid zinc complex. After mixing the two solutions, complex formation began about 1 s later. After 5 s, microcrystals were forming and moving. After about 15 s, the microcrystals had spread throughout the entire droplet and continued to move. After 120 s, the movement of the microcrystals stopped, and the chemical reaction was complete. Furthermore, the contact angle of the reaction solution with the water-repellent substrate was 121.7°, and the solution could be collected using a pipette after the reaction was completed.

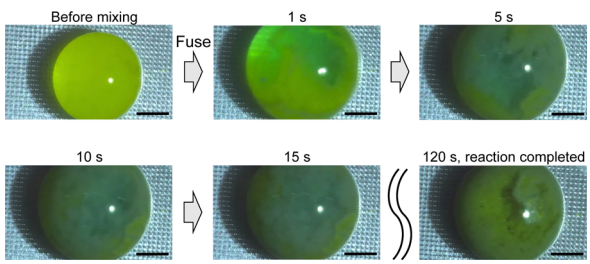

Fig. 9 Observation of the synthesis of a Zn(II) complex. 1 s: the chemical reaction begins as soon as the two reagents mix. 5 s: the metal complex begins to form. 10 s: microcrystals of the metal complex are dispersed in the droplet. 15 s: the reaction progresses as the microcrystals move within the droplet. 120 s: the movement of the microcrystals stops and the chemical reaction ends. Scale bar is 300 μm.

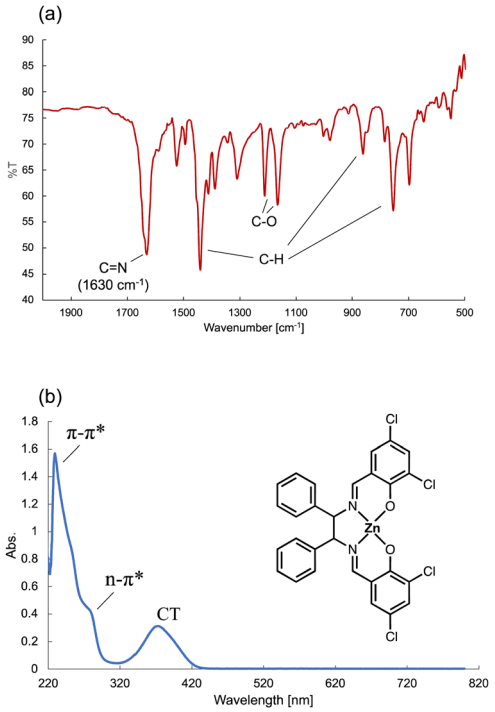

Fig. 10 Compound identification analysis. (a) IR spectrum. The peak near 1630 cm^{-1} is due to C═N bonds. (b) UV-vis spectrum, containing a π–π* transition at 225 nm, an n–π* transition 285 nm, and a CT transition around 400 nm.

Fig. 10(a) shows the IR spectrum of the Zn(II) complex. The C═N bond peak was observed at around 1630 cm^{-1}. Fig. 10(b) shows the UV-vis spectrum containing a π–π* transition at 225 nm, an n–π* transition 285 nm, and a charge transfer (CT) transition around 400 nm. The IR and UV-vis spectra confirmed that the Zn(II) complex had been synthesized on the water-repellent device. The synthesis of the Zn(II) complex using a beaker requires 2 h of thermal stirring at 40 °C to synthesize the ligand, and then another 2 h of thermal stirring at 40 °C after adding zinc acetate, whereas

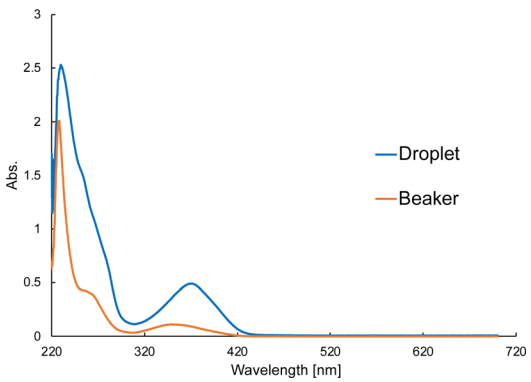

Fig. 11 UV-vis spectrum, comparison of product peak intensities between beaker and droplet.

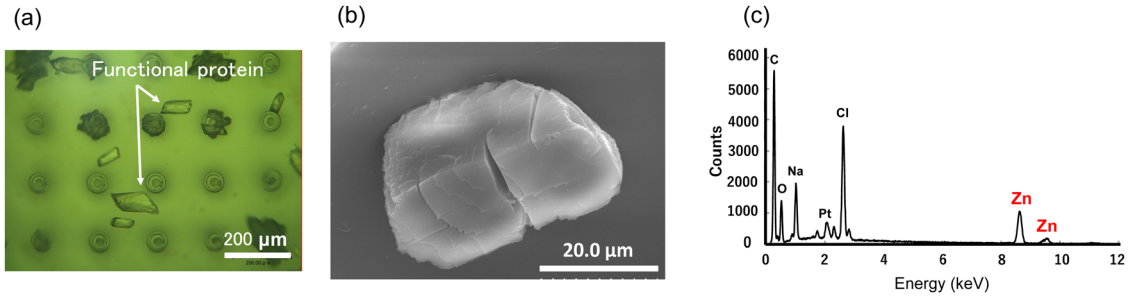

Fig. 12 Crystallization of Zn(II) complex-containing protein. (a) Optical microscope image of crystals. (b) SEM image of crystal. (c) Elemental analysis by EDX.

the synthesis was completed in about 120 s in the microdroplets. The solution on the water-repellent device is in the form of microdroplets, chemical reactions proceed more quickly than in a beaker because diffusion times for chemical species is faster in microdroplets than in beakers.[42] Fig. 11 shows a comparison of the peak intensity of the UV-vis spectrum for the beaker and droplets. The products in the beaker and droplets were similarly diluted and measurements were performed, but the peak intensity of the droplets was about 0.5 higher. This indicates that the concentration of the product in the droplet was higher than that in the beaker, and that it was synthesized in a high yield.

Synthesis and crystallization of a Zn(II) complex-containing protein

Fig. 12(a) shows an optical microscope image of the crystal growth of the Zn(II) complex-containing protein on the water-repellent device. Crystals about 100 μm in size are visible. Fig. 12(b) is an SEM image showing a single crystal of the Zn(II) complex-containing protein. Protein crystallization on a microscale produces high-quality crystals by suppressing convection caused by the concentration gradient of the crystallization solution that accompanies crystal growth.[11] In this experiment, microcrystals began to form 90 min after the start of crystallization, and large single crystals were obtained in about 120 min. In the crystallization experiment on the water-repellent device, a lid was placed over the microdroplet to prevent evaporation of the solution, but a small amount of evaporation likely still occurred from the surface of the microdroplet. The crystals formed quickly, probably because of the evaporation of water from the protein solution, which increased the protein concentration. Furthermore, including a poor solvent is also believed to have contributed to the rapid formation of crystals. Protein crystals can become distorted if the crystal growth rate is too fast, but we obtained large single crystals. The resulting crystals were collected using a pipette. After washing the crystal surface with pure water, elemental analysis was performed using EDX (Fig. 12(c)), and the peaks at 8.5 and 9.5 keV due to Zn confirmed that the Zn(II) complex was docked to the protein. The contact angle of the protein solution with the water-repellent substrate was 132.5°, and the protein crystals could be recovered using a pipette after crystallization was completed.

Conclusions

In this study, a soft MEMS technology easily fabricated an umbrella-shaped water-repellent device. The shape of the interface was clarified by simulating the shape of droplets of water and methanol on the device. The contact angles of methanol on the SU-8 substrate of 22.3° and the umbrella-shaped pillar array of 118.8° showed a large difference.

A Zn(II) complex was synthesized in microdroplets on a water-repellent pillar array. The chemical reaction in the microdroplets was observed with a high-speed camera. The product was easily collected by pipette and analysed for identification.

A metal complex and a protein containing a metal complex were synthesized and crystallized on umbrella-shaped water-repellent pillars. The product was extracted easily using a pipette. We obtained clean single crystals of the protein containing the metal complex and performed an elemental analysis of the crystals. In the future, we plan to perform structural analysis at a synchrotron radiation facility.

Using the water-repellent pillar array device for chemical synthesis decreased the reagents and eliminated the need for heating. Furthermore, the protein crystallization experiment obtained beautiful crystals characteristic of microdroplets. This shows that the device can be used in various chemical syntheses, from simple chemical reactions, such as metal complexes, to the synthesis of polymeric proteins. The water-repellent device developed in this study is expected to become a new platform for future chemical synthesis.

Author contributions

D. Tanaka: conceptualization, data curation, formal analysis, funding acquisition, methodology, project administration, verification, visualisation, writing – original draft. M. Kobayashi and R. Fujita: data curation, formal analysis, investigation, methodology, verification, visualisation, writing – original draft preparation. D. H. Yoon, T. Sekiguchi and T. Akitsu: formal analysis, methodology, validation, visualization. S. Shoji and T. Tanii: investigation, methodology. M. Furuya: formal analysis, funding acquisition, project administration, Writing – review & editing.

Data availability

The data that support the findings of this study are available from the corresponding authors upon reasonable request.

Conflicts of interest

There are no conflicts to declare.

Acknowledgements

This work was supported by JST, ACT-X Grant Number JPMJAX21KA, Japan, and JSPS KAKENHI Grant Number JP24K00912, No. JP23K13652. The authors thank for MEXT ARIM Japan (Advanced Research Infrastructure for Materials and Nanotechnology in Japan) of Waseda University. Proposal Number JPMXP1224WS0006.

References

1 M. Claudel, J. V. Schwarte and K. M. Fromm, *Chemistry*, 2020, **2**, 849.
2 C. Imberti, P. Zhang, H. Huang and P. J. Sadler, *Angew. Chem., Int. Ed.*, 2020, **59**, 61.
3 P. C. A. Bruijnincx and P. J. Sadler, *Curr. Opin. Chem. Biol.*, 2008, **12**, 197.
4 P. Lopes, K. Koschorreck, J. N. Pedersen, A. Ferapontov, S. Lörcher, J. S. Pedersen, V. B. Urlacher and E. E. Ferapontova, *ChemElectroChem*, 2019, **6**, 2043.
5 K. Das, S. Nandi, S. Mondal, T. Askun, Z. Canturk, P. Celikboyun, C. Massera, E. Garribba, A. Datta, C. Sinha and T. Akitsu, *New J. Chem.*, 2014, **39**, 1101.
6 N. Fani, A. K. Bordbar and Y. Ghayeb, *Spectrochim. Acta, Part A*, 2013, **103**, 11.
7 W. Nogala, K. Szot, M. Burchardt, F. Roelfs, J. Rogalski, M. Opalloa and G. Wittstock, *Analyst*, 2010, **135**, 2051.
8 B. Zheng, L. S. Roach and R. F. Ismagilov, *J. Am. Chem. Soc.*, 2003, **125**, 11170.
9 H.-H. Shi, Y. Xiao, S. Ferguson, X. Huang, N. Wang and H.-X. Hao, *Lab Chip*, 2017, **17**, 2167.
10 L. Li and R. F. Ismagilov, *Annu. Rev. Biophys.*, 2010, **39**, 139.
11 M. Maeki, S. Yamazaki, A. S. Pawate, A. Ishida, H. Tani, K. Yamashita, M. Sugishima, K. Watanabe, M. Tokeshi, P. J. A. Kenisd and M. Miyazaki, *CrystEngComm*, 2016, **18**, 7722.
12 M. Maeki, H. Tani, S. Ito, R. Takeda, G. Ueno, A. Ishida, M. Yamamoto and M. Tokeshi, *Chem. Sci.*, 2020, **11**, 9072.
13 J. Ferreira, F. Castro, F. Rocha and S. Kuhn, *Chem. Eng. Sci.*, 2018, **191**, 232.
14 Y. Zhu, L.-N. Zhu, R. Guo, H.-J. Cui, S. Ye and Q. Fang, *Sci. Rep.*, 2014, **4**, 5046.
15 A. A. Fedorets, S. Koltsov, A. A. Muravev, A. Fotin, P. Zun, N. Orekhov, M. Nosonovsky and E. V. Skorb, *Chem. Sci.*, 2024, **15**, 12067.
16 J. Jang, G. Coquerel, T. Seok Seo, W. S. Kim and B. J. Park, *Lab Chip*, 2024, **24**, 5055.
17 H. Song, D. L. Chen and R. F. Ismagilov, *Angew. Chem., Int. Ed.*, 2006, **45**, 7336.
18 A. Kalantarifard, A. Saateh and C. Elbuken, *Chemosensors*, 2018, **6**, 23.
19 K. Lv, A. W. Perriman and S. Mann, *Chem. Commun.*, 2015, **51**, 8600.
20 K. Hung Huang, Z. Wei and R. Graham Cooks, *Chem. Sci.*, 2021, **12**, 2242.
21 M. Li, S. Yang, M. Rathi, S. Kumar, C. S. Dutcher and V. H. Grassian, *Chem. Sci.*, 2024, **15**, 13429.
22 S. Mashaghi and A. M. van Oijen, *Sci. Rep.*, 2015, **5**, 11837.
23 C. K. T. Weatherly, M. W. Glasscott and J. E. Dick, *Langmuir*, 2020, **36**, 8231.
24 H. Kim, K.-I. Min, K. Inoue, D. J. Im, D.-P. Kim and J. Yoshida, *Science*, 2016, **352**, 691.
25 T. Fukuda, N. Funaki, T. Kurabayashia, M. Suzuki, D. H. Yoon, A. Nakahara, T. Sekiguchi and S. Shoji, *Sens. Actuators, B*, 2014, **203**, 536.
26 M. Neumann and K. Zeitler, *Org. Lett.*, 2012, **14**, 2658.
27 D. Stanssens, H. Van den Abbeele, L. Vonck, G. Schoukens, M. Deconinck and P. Samyn, *Mater. Lett.*, 2011, **65**, 1781.
28 M. Fukuyama, M. Tokeshi, M. A. Proskurnin and A. Hibara, *Lab Chip*, 2018, **18**, 356.
29 J. E. Mates, I. S. Bayer, J. M. Palumbo, P. J. Carroll and C. M. Megaridis, *Nat. Commun.*, 2015, **6**, 8874.
30 T. Hao, K. Wang, Y. Chen, X. Ma, Z. Lan and T. Bai, *Ind. Eng. Chem. Res.*, 2018, **57**, 4452.
31 B. Su, S. Wang, Y. Song and L. Jiang, *Nano Res.*, 2011, **4**, 266.
32 X.-T. Luo and C.-J. Li, *Small*, 2019, **15**, 1901919.
33 D. Chandra and S. Yang, *Acc. Chem. Res.*, 2010, **43**, 1080.
34 M. Lejeune, T. Chartier, C. Dossou-Yovo and R. Noguera, *J. Eur. Ceram. Soc.*, 2009, **29**, 905.
35 L. Gustafsson, R. Jansson, M. Hedhammar and W. van der Wijngaart, *Adv. Mater.*, 2018, **30**, 1704325.
36 X. Liu, H. Gu, M. Wang, X. Du, B. Gao, A. Elbaz, L. Sun, J. Liao, P. Xiao and Z. Gu, *Adv. Mater.*, 2018, **30**, 1800103.
37 N.-E. Oyunbaatar, D.-H. Lee, S. J. Patil, E.-S. Kim and D.-W. Lee, *Sensors*, 2016, **16**, 1258.
38 I. Fujii and N. Hirayama, *Acta Cryst.*, 1999, **55**, 1247.
39 R. M. Bain, C. J. Pulliam, F. Thery and R. G. Cooks, *Angew. Chem., Int. Ed.*, 2016, **55**, 10478.
40 K. Li, K. Gong, J. Liu, L. Ohnoutek, J. Ao, Y. Liu, X. Chen, G. Xu, X. Ruan, H. Cheng, J. Han, G. Sui, M. Ji, V. K. Valev and L. Zhang, *Cell Rep. Phys. Sci.*, 2022, **3**, 100917.
41 T. Liu and C.-J. Kim, *Science*, 2014, **346**, 6213.
42 D. Tanaka, S. Sawai, S. Hattori, Y. Nozaki, D. H. Yoon, H. Fujita, T. Sekiguchi, T. Akitsu and S. Shoji, *RSC Adv.*, 2020, **10**, 38900.